Transient and Temperature Response of a Distributed, Thermally Activated System*

J. Ross Macdonald
Texas Instruments Incorporated, Dallas 22, Texas
(Received 14 May 1962; in final form 15 October 1962)

After a brief survey of methods of representing the transient response of a distributed linear system, a general analysis is presented of the temperature dependence of relaxation times of a thermally activated system. It is assumed that either the pre-exponential factor τ_d (or its inverse, the vibrational frequency ν_d) or the activation energy E may be separately distributed or that they both depend linearly on a structure factor S and so are similarly distributed. Further, τ_d, E, and parameters of their distributions are taken temperature independent. A two-parameter, generalized, truncated exponential probability density function is chosen for the distribution of S and transformed to yield a power-law distribution for $G(\tau)$, the over-all relaxation-time distribution function. Expressions yielding the time and temperature response of the system are then derived from $G(\tau)$. The specific transient response considered is that following the imposition of a constant forcing function at $t=0$ and may represent the charge and current response of a dielectric system after application or removal of a constant voltage, the strain and rate-of-strain response of a mechanical system after constant stress is applied or removed, or the stress and rate-of-stress response on application and maintenance of a constant strain. Representative results are found to agree quantitatively or qualitatively with available transient and temperature responses for a wide variety of materials under electrical or mechanical stimulation. In particular, the current transient response or stress relaxation response is constant for measuring times less than the shortest relaxation time of the system, then exhibits one or two regions with $t^{-(1+p_i)}$ behavior, and, finally, decreases very rapidly when the measuring time exceeds the longest time constant of the system. The theory leads to specific possibilities for the temperature behavior of p_i and to reasons why it is usually found to be less than unity in magnitude. Finally, conditions are analyzed for which the time–temperature superposition law of rheology applies.

I. INTRODUCTION

MANY approaches have been used to deal with a linear system whose measurable response extends over a relatively wide range of times or frequencies. Since a detailed microscopic theory leading unambiguously to a continuous or discontinuous distribution of relaxation (or retardation) times (abbreviated hereafter as DRT) is usually unavailable for all but the simplest systems, it has been customary to introduce a relaxation-time distribution (RTD) heuristically. Most such phenomenological distributions involve a single shape parameter which is adjusted to yield the best fit between theory and experiment. In the present work, we only distinguish between retardation and relaxation times and systems when necessary and shall usually use relaxation as the inclusive term.

Three different methods have been used to derive forms for phenomenological relaxation-time distribution functions (RTDF). These methods differ only in that initial attention is focussed on the frequency, the time, or the relaxation-time domains. Results obtained in any one of these domains can be transformed to the other.[1] The Fuoss–Kirkwood,[2] Cole–Cole,[3] and Davidson–Cole[4] distributions were derived by introducing a disposable parameter into frequency-response functions. The Wagner[5,6] DRT, however, was selected directly on the basis of physical plausibility. Finally, a number of DRT's have been obtained by induction from the form of the transient response of the system.[7,8] In spite of much consideration of various kinds of RTDF's in prior theoretical work, very little attention has been given to the temperature dependence of their parameters and the resulting effect on temperature dependence of system transient and frequency response. Such analysis is one of the main aims of the present work.

Although many dielectric and mechanical relaxation measurements point to relaxation frequencies which obey an Arrhenius or closely allied equation and are thus associated with a thermally activated process, of the above distributions only that of Wagner can be made consistent with a distribution of activation energies (DAE) or with simultaneously present distributions of activation energy and pre-exponential factor in an Arrhenius equation.[9–11] However, the Wagner RTDF is a distribution symmetrical in $\ln(\tau/\tau_0)$, where τ_0 is the most probable relaxation time, and cannot, therefore, represent data well which require an unsymmetrical distribution. Therefore, in the present work we consider the transient response associated with another[9,10] simpler RTDF which is also consistent with a thermally acti-

* Presented in part at the Baltimore, Maryland annual meeting of the Society of Rheology, 29 October 1962.

[1] J. R. Macdonald and M. K. Brachman, Revs. Mod. Phys. **28**, 393 (1956).

[2] R. M. Fuoss and J. G. Kirkwood, J. Am. Chem. Soc. **63**, 385 (1941).

[3] K. S. Cole and R. H. Cole, J. Chem. Phys. **9**, 341 (1941).

[4] D. W. Davidson and R. H. Cole, J. Chem. Phys. **19**, 1484 (1951).

[5] K. W. Wagner, Ann. Physik **40**, 817 (1913).

[6] W. A. Yager, Physics **7**, 434 (1936).

[7] G. M. Voglis, Z. Physik **109**, 52 (1938).

[8] J. R. Macdonald, J. Appl. Phys. **32**, 2385 (1961).

[9] J. R. Macdonald, J. Chem. Phys. **36**, 345 (1962); Bull. Am. Phys. Soc. **6**, 449 (1961).

[10] J. R. Macdonald, Physica **28**, 485 (1962).

[11] A. S. Nowick and B. S. Berry, IBM J. Res. Develop. **5**, 297, 312 (1961).

vated process, which can be either symmetrical or unsymmetrical, and which can yield results in good agreement with much experimental data. The frequency response associated with the present distribution will be discussed in a further paper.[12]

In the next section, a general survey of distributed, linear system transient response is given, followed by a discussion of the temperature response of relaxation times for a thermally activated system. Various possibilities for distributed character are subsumed in a single representation of considerable generality, and specific transient and temperature response functions are derived and discussed after selection of a physically reasonable probability-density distribution function.

II. GENERAL TRANSIENT RESPONSE

In the present work, the transient response is calculated for a dielectric system, but the results apply as well to transient effects in many other linear systems, such as mechanical creep and stress relaxation. A detailed comparison between such systems has been given elsewhere.[13] Let us now consider a guarded capacitor whose capacitance is C_m when its dielectric is the material to be measured and is C_a for an air or vacuum dielectric. Let ϵ_a be the dielectric constant of air, and ϵ_s and ϵ_∞ be the values of the real part of the dielectric constant of the material studied at limiting low (static) and high frequencies, respectively. Then the current which flows in the initially uncharged material capacitor when a voltage $V(t)$ is applied at $t=0$ will be, from the superposition principle,[1,13]

$$i(t)=\left(\frac{C_a}{\epsilon_a}\right)\left[\epsilon_\infty\frac{dV}{dt}+(\epsilon_s-\epsilon_\infty)\int_{0-}^{t+}\frac{dV(x)}{dx}A(t-x)dx\right], \quad (1)$$

where $A(t)$ is here the indicial admittance of the system exclusive of instantaneous-response terms and is zero for $t<0$, $u_0(t)$ is the unit step function, and $\epsilon=(\epsilon_a/C_a)C_m$. The quantity $A(t)$ will be related to a RTDF later. The charge $q(t)$ is just

$$q(t)=\int_{0-}^{t} i(x)dx. \quad (2)$$

Although quantities such as $i(t)$, $A(t)$, and $q(t)$ depend on temperature as well as time, such full dependence will usually not be explicitly indicated.

We shall be primarily interested in an input voltage of the form $V(t)\equiv V_0u_0(t)$, where V_0 is a constant voltage. Its introduction in (1) leads to

$$i(t)=V_0[C_\infty\delta(t)+(C_s-C_\infty)A(t)], \quad (3)$$

where C_∞ and C_s refer to the capacitor with material dielectric and $\delta(t)$ is the Dirac delta function, formally equal to $d[u_0(t)]/dt$. Equation (3) shows that $A(t)$ specifies the characteristic transient response of the system when the input is a constant voltage V_0 applied suddenly at $t=0$. Although there will usually be some temperature dependence of (C_s-C_∞), this dependence[14,15] is independent of $A(t)$ and the normalized RTDF and can frequently be separately measured. The charge in the present case is

$$q(t)=V_0[C_\infty u_0(t)+(C_s-C_\infty)\psi(t)], \quad (4)$$

where

$$\psi(t)\equiv\int_{0-}^{t}A(x)dx \quad (5)$$

and $\psi(t)=0$ for all $t<0$.

Since $q(t)=C_m(t)V(t)$, (4) shows that for step function response

$$\psi(t)=\frac{C_m(t)-C_\infty}{C_s-C_\infty}u_0(t)=\frac{\epsilon(t)-\epsilon_\infty}{\epsilon_s-\epsilon_\infty}u_0(t), \quad (6)$$

where $\epsilon(t)$ is the time-varying effective dielectric constant. Note that $\psi(0)=0$ and $\psi(\infty)=1$. Thus, the final charge is C_sV_0. The quantity ψ is called the creep retardation function in the mechanical retardation case and is a measure of the creep strain under constant stress.[8,13] A further quantity, $\phi(t)\equiv u_0(t)-\psi(t)$, may be defined which will represent the relaxation, or approach to equilibrium, of a retardation system on removal of a stimulus such as constant stress after equilibrium under the stimulus has been attained. When a relaxation system is considered, however, $\phi(t)\equiv u_0(t)-\psi(t)$ may be used to describe, e.g., the relaxation of stress after the application and maintenance of constant strain. When both strain retardation and stress relaxation measurements are made on the same material, the ϕ representing relaxation of the strain after removal of stress is related to but not equal to that representing the relaxation of stress under constant strain. In these two situations, the distribution of retardation times is not equal to the distribution of relaxation times, and thus the ϕ's derived from them are different.

Sometimes dielectric measurements are made by applying a ramp voltage $V(t)=\alpha t u_0(t)$, where α is a constant.[16] In this case, Eq. (1) leads to

$$i(t)=\alpha[C_\infty u_0(t)+(C_s-C_\infty)\psi(t)]. \quad (7)$$

Although the dimensions are different, this result is formally equivalent to (4). Since it is frequently more convenient to measure a current than a charge, the ramp-voltage method is often used in place of charge measurement to obtain the function $\psi(t)$. In creep measurements $\psi(t)$ can, of course, be determined directly from measured strain under constant load.

[12] J. R. Macdonald (in preparation).
[13] J. R. Macdonald and C. A. Barlow, Jr., Revs. Mod. Phys. (to be published).
[14] J. R. Macdonald and C. A. Barlow, Jr., J. Chem. Phys. **36**, 3062 (1962).
[15] B. E. Read and G. Williams, Trans. Faraday Soc. **57**, 1979 (1961).
[16] D. W. Davidson, R. P. Auty, and R. H. Cole, Rev. Sci. Instr. **22**, 678 (1951).

In actual measurements of dielectric transient response, the discharge current (after full charging) is often measured instead of the charging current. When the system is linear and there is no dc conduction or its effect is subtracted from the data, the magnitudes of these currents are equal at equal times after the beginning of charge and discharge, and we may write[13] $A_d(t)\equiv -A_c(t)$ for $t>0$ and $\phi_d(t)\equiv u_0(t)-\psi_c(t)$, using the superscripts d and c to indicate discharge and charge. In many experiments, however, the dielectric is charged at constant voltage for a finite time t_0, then discharged through essentially a short circuit. In this case, the applied voltage is $V(t)=V_0[u_0(t)-u_0(t-t_0)]$ and the corresponding discharge current involves the function

$$D_0(t)\equiv A(t)-A(t-t_0) \tag{8}$$

instead of $A(t)$. In order to evaluate the effect of a finite charging interval, it is of interest to compare the discharge current after such a finite charging period to that for a infinite interval (or the charging current starting from a completely uncharged condition). If we now measure time from the beginning of the discharge and change the sign of $D_0(t)$ to allow direct comparison with the charging current of (3), we obtain the function

$$D(t)=A(t)-A(t+t_0)u_0(t), \tag{9}$$

which is compared directly with $A(t)$.

In the limit of short charging times, the applied voltage begins to approximate an impulse or non-normalized delta function. Therefore, the response of the system to $V(t)=\Lambda_0\delta(t)$ is of interest. From (1) the current response is

$$i(t)=\Lambda_0[C_\infty\delta'(t)+(C_s-C_\infty)\{dA(t)/dt\}], \tag{10}$$

where $\delta'(t)$ is the first derivative of the delta function. Thus, dA/dt rather than $A(t)$ is involved in the response in this case.

III. TEMPERATURE CONSIDERATIONS

In the present analysis, we shall be solely concerned with thermally activated relaxation processes.[10,17,18] In previous work,[10] it has been shown that physically reasonable assumptions concerning the temperature dependence of the potential barrier height involved in an individual relaxation process lead to the frequently found experimental situation of a temperature independent heat of activation, or activation energy E and entropy increment $\Delta S=E/\theta_0$, where θ_0 is an absolute temperature usually above that experimentally possible without phase or structure change.[18a] On introducing the normalized activation energy $\mathcal{E}\equiv E/k\theta_n$, one then finds[10] that an individual relaxation time τ may be expressed as

$$\tau=\tau_d\exp(\eta\mathcal{E}), \tag{11}$$

where $\eta\equiv(\theta_n/\theta)-(\theta_n/\theta_0)$, θ_n is an arbitrary normalization temperature, and $\tau_d\equiv\nu_d^{-1}$ is an attack time or inverse vibrational frequency, the limiting value of τ when $\theta=\theta_0$.

Although τ_d may sometimes be a slowly varying function of temperature,[9,10,19] for concreteness we shall here take it as temperature independent. Both τ_d and $\mathcal{E}$ may be distributed, and we make the physically plausible assumption[9] that when these quantities are themselves temperature independent, their distributions are also temperature independent. Let us designate the extreme values of τ_d and $\mathcal{E}$ which appear when they are distributed as τ_{d1}, τ_{d2}, and $\mathcal{E}_1$, $\mathcal{E}_2$, respectively. We may next define $\tau_{dc}\equiv(\tau_{d1}\tau_{d2})^{\frac{1}{2}}$ and $\mathcal{E}_c\equiv(\mathcal{E}_1+\mathcal{E}_2)/2$. When τ_d and $\mathcal{E}$ are not distributed, their values are τ_{dc} and $\mathcal{E}_c$, since in this case $\tau_{d1}=\tau_{d2}=\tau_{dc}$ and $\mathcal{E}_1=\mathcal{E}_2=\mathcal{E}_c$.

We shall only be concerned with the cases where either the variable $\mathcal{L}\equiv\ln(\tau_d/\tau_{dc})$, or $\mathcal{E}$, or both depends linearly on a single, temperature-independent, distributed structure variable $\mathcal{S}$, whose range extends from $\mathcal{S}_1$ to $\mathcal{S}_2$. In any of these cases, where $\mathcal{E}$ has a specific value, $\mathcal{S}$ will have a fixed or related value. We may thus write from (11)

$$\tau_c=\tau_{dc}\exp(\eta\mathcal{E}_c), \tag{12}$$

where τ_c is some "central" relaxation time satisfying $\tau_c=(\tau_1\tau_2)^{\frac{1}{2}}$ and

$$\tau_i=\tau_{di}\exp(\eta\mathcal{E}_i) \tag{13}$$

for $i=1, 2$.

The combination of (11) and (12) yields

$$s\equiv\ln(\tau/\tau_c)=\mathcal{L}+\eta(\mathcal{E}-\mathcal{E}_c). \tag{14}$$

Let us now take[10,11] $\mathcal{L}=\alpha_1+\beta_1\mathcal{S}$ and $\mathcal{E}=\alpha_2+\beta_2\mathcal{S}$, where the α's and β's are temperature-independent constants. Substitution in (14) and the use of $s_c=0$ yields

$$\begin{aligned} s&=[\beta_1+\eta\beta_2][\mathcal{S}-\mathcal{S}_c] \\ &\equiv\gamma^{-1}x, \end{aligned} \tag{15}$$

where $x\equiv(\mathcal{S}-\mathcal{S}_c)$, and $\mathcal{S}_c=-\alpha_1/\beta_1$ when $\beta_1\neq 0$. Note that β_1 and β_2 may be individually positive or negative. Without significant loss of generality, we shall take $\beta_2\geq 0$ hereafter. When $\beta_2>0$ and $\beta_1>0$, $\mathcal{L}$ and $\mathcal{E}$ will then be distributed similarly, but when $\beta_2>0$ and $\beta_1<0$, the variable $-\mathcal{L}\equiv\ln(\nu_d/\nu_{dc})$ and $\mathcal{E}$ will have similar distributions.[10] Since $\mathcal{E}_2\geq\mathcal{E}_1$, the choice $\beta_2\geq 0$ requires that $\mathcal{S}$ also be greater than or equal to $\mathcal{S}_1$ when $\beta_2\neq 0$, and we therefore always take $\mathcal{S}_2\geq\mathcal{S}_1$.

When $\beta_1=0$, $\tau_d=\tau_{dc}$, and τ_d is not distributed. Similarly, when $\beta_2=0$, $\mathcal{E}=\mathcal{E}_c$ and $\mathcal{E}$ is not distributed. When $\beta_2\neq 0$, the case of greatest interest and the one

[17] C. Zener, *Imperfections in Nearly Perfect Crystals*, edited by W. Shockley *et al.* (John Wiley & Sons, Inc., New York, 1952), p. 289 ff.

[18] D. Lazarus, *Solid State Physics*, edited by F. Seitz and D. Turnbull (Academic Press Inc., New York, 1960), Vol. 10, p. 115.

[18a] *Note added in proof.* The relation $\Delta S/E=$constant has also been derived by a different method and considered in more detail by A. W. Lawson [J. Chem. Phys. **32**, 131 (1960)].

[19] R. H. Doremus, J. Chem. Phys. **34**, 2186 (1961).

we consider in most detail, we may rewrite (15) as

$$s=[(\beta_1/\beta_2)+\eta][\mathcal{E}-\mathcal{E}_c]$$
$$=(\beta_2\gamma)^{-1}[\mathcal{E}-\mathcal{E}_c]\equiv\sigma[\mathcal{E}-\mathcal{E}_c], \quad (16)$$

where σ is a new inverse temperature variable. By considering all temperature dependence in terms of σ instead of θ_n/θ, we can include all combinations of (β_1/β_2) and η automatically and change from one set of conditions to another by a simple translation of results along the σ axis. The combination of (12) and (16) finally yields

$$\tau=\tau_{dc}\exp[-(\beta_1/\beta_2)\mathcal{E}_c+\sigma\mathcal{E}]. \quad (17)$$

When $\gamma=\infty$, either because $\sigma=0$ or because $\beta_1=\beta_2=0$, Eq. (15) shows that $\tau=\tau_1=\tau_2=\tau_c\equiv\tau_{c\infty}$; there is then only a single effective relaxation time in the system and it exhibits simple Debye dispersion. When $\beta_2\neq0$, the condition $\sigma=0$ is only physically realizable when the corresponding temperature θ_∞ satisfies $\theta_\infty>0$, where θ_∞ is defined by $(\theta_n/\theta_\infty)\equiv(\theta_n/\theta_0)-(\beta_1/\beta_2)$. The value of τ_c at this temperature is then

$$\tau_{c\infty}=\tau_{dc}\exp(\eta_\infty\mathcal{E}_c)=\tau_{dc}\exp[-(\beta_1/\beta_2)\mathcal{E}_c]. \quad (18)$$

For calculation purposes, it is desirable to define a normalized time variable $Y\equiv t/\tau_c$. However, this quantity depends on temperature as well when $\mathcal{E}_c\neq0$; thus, to allow convenient comparison between theory and experiment we may define the temperature-independent time variable $T\equiv t/\tau_{cn}=RY$, where $R\equiv\tau_c/\tau_{cn}$ and τ_{cn} is the value of τ_c from (12) evaluated at $\theta=\theta_n$. When $\theta=\theta_n$, $\sigma=\sigma_n\equiv(\beta_1/\beta_2)+\eta_n$, where $\eta_n\equiv1-(\theta_n/\theta_0)$. The quantity R may be written

$$R=\exp[(\theta_n-\theta)\mathcal{E}_c/\theta]\doteq\exp[(\sigma-\sigma_n)\mathcal{E}_c], \quad (19)$$

which depends on temperature only through σ when $\beta_2\neq0$.

Finally, let us introduce the normalized relaxation-frequency variable $z\equiv\tau_c/\tau=\exp(-s)$. The relation[1,8] between $A(t)$ and a RTDF $G(\tau)$ may now be expressed in terms of the above variable as

$$A(t)=A(\tau_cY)$$
$$=u_0(t)\int_{z_{\min}-}^{z_{\max}+}z^{-1}G(\tau_cz^{-1})\exp(-Yz)dz, \quad (20)$$

where $z_{\min}$ and $z_{\max}$ are the smallest and largest values of z, given by τ_c/τ_2 and τ_c/τ_1, respectively, for $\sigma>0$ and interchanged for $\sigma<0$. The limits are written $z_{\max}+$ and $z_{\min}-$ to include the full contribution from any δ-function terms present.[13] An important temperature-independent quantity is $r\equiv\exp[\mathrm{sgn}\delta(\mathcal{J}_2-\mathcal{J}_1)/2]$, where $\delta\equiv\beta_2$ and $\mathcal{J}\equiv\mathcal{E}$ when $\beta_2\neq0$, while $\delta\equiv\beta_1$, $\mathcal{J}\equiv\mathcal{L}$ when $\beta_2=0$. When τ_c is taken as $(\tau_1\tau_2)^{\frac{1}{2}}$, $z_{\max}=z_{\min}^{-1}=(\tau_2/\tau_1)^{(\mathrm{sgn}\gamma)\frac{1}{2}}$, equal to $r^{|\sigma|}$ when $\beta_2\neq0$ and to r when $\beta_2=0$. Here, $\mathrm{sgn}\gamma\equiv\gamma/|\gamma|$; $\mathrm{sgn}0\equiv0$. Thus r^2 is the ratio of maximum to minimum time constants of the system when $\beta_2=0$ and is this ratio at the temperature specified by $\sigma=1$ when $\beta_2\neq0$.

Throughout the present work, we use a RTDF normalized to unity. The normalization condition may be expressed as

$$\tau_c\int_{z_{\min}-}^{z_{\max}+}z^{-2}G(\tau_cz^{-1})dz=1. \quad (21)$$

This condition, plus Eq. (5), leads to

$$\psi(t)=\psi(\tau_cY),$$
$$=u_0(t)\left[1-\tau_c\int_{z_{\min}-}^{z_{\max}+}z^{-2}G(\tau_cz^{-1})\exp(-Yz)dz\right],$$
$$\equiv u_0(t)-\phi(t). \quad (22)$$

IV. SPECIFIC RELAXATION-TIME DISTRIBUTION

In this section, we obtain a RTDF by first selecting a reasonable probability density function for the normalized structure variable $\mathcal{S}$. Pearson has derived a large number of types of probability distributions, which are summarized by Elderton.[20] One of the most interesting is the gamma distribution, which includes the χ^2 and exponential distributions as special cases and has been used[21] as a statistical model for the life-length of materials. Here, we use the exponential distribution, modify it slightly for greater generality, and apply it over a finite range. Some further discussion of the physical applicability of the exponential distribution for the present situation and for life testing has been given elsewhere.[10,22]

If $\mathcal{S}_1$ and $\mathcal{S}_2$ are minimum and maximum values of $\mathcal{S}$, respectively, the condition $\tau_c=(\tau_1\tau_2)^{\frac{1}{2}}$ leads to $\mathcal{S}_c\equiv(\mathcal{S}_1+\mathcal{S}_2)/2$. We now pick the probability density of $x\equiv\mathcal{S}-\mathcal{S}_c$ as

$$p_x(x)=N\begin{cases}\exp(-\lambda_1x) & x_1\leqslant x\leqslant0\\ \exp(-\lambda_2x) & 0\leqslant x\leqslant x_2\end{cases} \quad (23)$$
$$=0 \qquad x<x_1,\quad x>x_2,$$

where N is the normalization factor for normalization to unity and λ_1 and λ_2 are temperature-independent constants which need not be equal. When they are equal and nonzero, one obtains the ordinary exponential distribution for a finite range. When they are both zero, (23) reduces to the well-known box distribution for which each value of $\mathcal{S}$ between $\mathcal{S}_1$ and $\mathcal{S}_2$ is equally probable.[23] The present introduction of separate λ_1 and λ_2 values allows $p_x(x)$ to be made symmetrical around $x=0$ by taking $\lambda_2=-\lambda_1$. Further, as becomes evident later, the present choice may lead to transient response of the form t^{-n} with

[20] W. P. Elderton, *Frequency Curves and Correlation* (Cambridge University Press, Cambridge, England, 1938), 3rd edition.
[21] Z. W. Birnbaum and S. C. Saunders, J. Am. Stat. Assoc. **53**, 151 (1958).
[22] D. J. Davis, J. Am. Stat. Assoc. **47**, 113 (1952).
[23] A. Matsumoto and K. Higasi, J. Chem. Phys. **36**, 1776 (1962); a number of further references concerning the box and generalized distributions are given in references 9, 30, and 31.

two different values of n in different time intervals, in agreement with considerable experimental data.[7,24–28] Finally, it may be used to approximate or sometimes duplicate the wedge-box distribution frequently employed in describing the mechanical relaxation of polymers.[29,30] It is worth pointing out that although (23) is quite general, it is not as general as possible for the present form of dependence. The present form is restricted by taking the point at which the two parts join at $\mathcal{S}=\mathcal{S}_c=(\mathcal{S}_1+\mathcal{S}_2)/2$. More generally, this point can occur anywhere between $\mathcal{S}_1$ and $\mathcal{S}_2$, and one could even interpose a region of zero probability density between the two separate nonzero parts. In the interests of simplicity and minimization of disposable parameters, we have dispensed with such additional freedom herein. Further generality could, of course, also be achieved by splitting up $p_x(x)$ into more than two nonzero parts. The introduction of many λ_i values and transition points would allow fitting of more complicated experimental curves but is usually unnecessary.

Next, we take $f(s)$ as the probability density for the logarithmic variable s. Then, we may write $G(\tau)|d\tau|=f(s)|ds|=p_x(x)|dx|$. This result, together with (15) and (23) then leads to

$$G(\tau)=G(\tau_c z^{-1})=B(\tau_{cn}R)^{-1}\begin{cases} & 1\leqslant z\leqslant b \quad (\gamma>0)\\ z^{1+\rho_1} & b\leqslant z\leqslant 1 \quad (\gamma<0)\\ & a\leqslant z\leqslant 1 \quad (\gamma>0)\\ z^{1+\rho_2} & 1\leqslant z\leqslant a \quad (\gamma<0)\end{cases}$$
$$=0 \qquad z<z_{\min},\ z>z_{\max}, \quad (24)$$

where $B\equiv|\gamma|N$, $b=a^{-1}\equiv\tau_c/\tau_1=\tau_2/\tau_c=(\tau_2/\tau_1)^{\frac{1}{2}}=r^{\sigma\operatorname{sgn}\beta_2}$ or $r^{\operatorname{sgn}\beta_1}$ when $\beta_2=0$, and

$$B\equiv\operatorname{sgn}\gamma\{\rho_1^{-1}(b^{\rho_1}-1)+\rho_2^{-1}(1-a^{\rho_2})\}^{-1}$$
$$=|\gamma|[\lambda_1^{-1}(r^{\xi_1\operatorname{sgn}\delta}-1)+\lambda_2^{-1}(1-r^{-\xi_2\operatorname{sgn}\delta})]^{-1}, \quad (25)$$

$$\xi_i\equiv\lambda_i\delta^{-1}, \quad (26)$$

$$\rho_i\equiv\lambda_i/(\beta_1+\beta_2\eta)=\lambda_i\gamma, \quad (27)$$

where ξ_1 is temperature independent, as is the term in square brackets in (25) which is also always greater than zero. Note that when $\beta_2=0$ with $\beta_1\neq 0$, $\rho_i=\xi_i$, while $\rho_i=\xi_i/\sigma$ when $\beta_2\neq 0$. Also, when $\beta_2\neq 0$ and $\rho_1=\rho_2=0$, $B=[|\sigma|(\mathcal{S}_2-\mathcal{S}_1)]^{-1}$.

By consideration of the form of $p_x(x)$ or $G(\tau)$, it can be shown that these quantities approach δ functions in certain limits.[10] Results for $G(\tau)$ are presented in Table I. Note that infinite values of ρ_i arise in the first four cases because a corresponding λ_i is infinite; in the last case, the condition $\gamma=\infty$ leads to infinite $|\rho_i|$.

TABLE I. Values of $G(\tau)$ in certain limits. $(-\infty<L\leq\infty)$.

$0<\lvert\gamma\rvert<\infty$		
ρ_1	ρ_2	$G(\tau)$
$-L$	$-\infty$	$\delta(\tau-\tau_2)$
∞	$-\infty$	$\frac{1}{2}[\delta(\tau-\tau_1)+\delta(\tau-\tau_2)]\,(x_1=-x_2)$
$-\infty$	∞	$\delta(\tau-\tau_c)$
∞	L	$\delta(\tau-\tau_1)$
$\gamma=\infty$,	$\lvert\rho_i\rvert=\infty$	$\delta(\tau-\tau_{c\infty})$

The present power-law distribution of Eq. (24) may be used in connection with either a retardation or relaxation situation,[13] but even with $\rho_1=\rho_2\equiv\rho$ has not previously been considered[23,31,32] in detail for a finite range and for arbitrary or temperature-dependent ρ_i. It is quite similar, however, to the truncated gamma distribution in z previously used to describe creep and mechanical dispersion in solids.[8] This distribution, which we here term the Karapetoff–Voglis[7,33] distribution (the K–V distribution) after those who first applied it for dielectric dispersion applications, becomes, when truncated at $\tau_{\max}\equiv\tau_2$,

$$G(\tau)=G(\tau_c z^{-1})=(\tau_{cn}R)^{-1}[\Gamma(-\nu,a)]^{-1}e^{-z}z^{1-\nu}$$
$$a\leq z\leq\infty$$
$$=0 \qquad z<a, \quad (28)$$

where ν is here a positive or negative shape parameter and $\Gamma(-\nu,a)$ is the tabulated[34] incomplete gamma function. The presence of the $\exp(-z)$ factor keeps the above result from being made entirely consistent with a temperature-independent distribution of $\mathcal{E}$ or of $\mathcal{E}$ and $\mathcal{L}$. However, it acts as a built-in truncation for $z>3$ or so. Thus, the effective range of τ is about $(\tau_c/3)<\tau<\tau_2$. It is evident that (28) will therefore yield results at a fixed temperature very similar to those of (24) for the special case $\rho_1\equiv\rho_2=\rho=-\nu$.

In (28), truncation at $\tau=\tau_{\max}$ or some similar change is necessary[8,35] to permit normalization for positive as well as negative values of ν. The untruncated K–V or gamma distribution in z has also been used to describe the response of polymers in their linear range.[36] Because even the truncated K–V distribution is only consistent with a distribution of $\mathcal{L}$, it is preferable to use the distribution of (24) in place of it whether $\mathcal{L}$, $\mathcal{E}$, or $\mathcal{E}$ and $\mathcal{L}$

[24] E. von Schweidler, Ann. Physik **24**, 711 (1907).
[25] K. S. Cole and R. H. Cole, J. Chem. Phys. **10**, 98 (1942).
[26] R. Gerson and J. H. Rohrbaugh, J. Chem. Phys. **23**, 2381 (1955).
[27] R. J. Munick, J. Appl. Phys. **27**, 1114 (1956).
[28] F. Cardon, Physica **27**, 841 (1961).
[29] A. V. Tobolsky, J. Am. Chem. Soc. **74**, 3786 (1952).
[30] A. V. Tobolsky, *Properties and Structure of Polymers* (John Wiley & Sons, Inc., New York, 1960), p. 123 ff.
[31] K. Higasi, *Dielectric Relaxation and Molecular Structure* (Monograph No. 9, Research Institute of Applied Electricity, Hokkaido University, Sapporo, Japan, 1961), Chap. II.
[32] W. E. Vaughan, W. S. Lovell, and C. P. Smyth, J. Chem. Phys. **36**, 753 (1962).
[33] V. Karapetoff, Elect. Eng. **45**, 236 (1926). It is worth noting that the first suggestion for use of the $\psi(t)$ function which follows from the untruncated K–V distribution[8] seems to be that of P. Kobeko, E. Kuvshinskij, and G. Gurevich, Zh. Tekh. Fiz. **4**, 622 (1937).
[34] K. Pearson, *Tables of the Incomplete Γ-Function* (Cambridge University Press, Cambridge, England, 1957).
[35] J. R. Macdonald, J. Appl. Phys. **30**, 453 (1959).
[36] A. V. Tobolsky and J. R. McLoughlin, J. Polymer Sci. **8**, 543 (1952).

are expected to be distributed. At a given temperature, the RTDF of (24) should well describe any data, either relaxation or retardation,[13] for which the truncated or untruncated K–V distribution has been used and should describe temperature dependence as well if the present assumption of a temperature independent $p_x(x)$ holds.

V. SPECIFIC TRANSIENT RESPONSES

When Eqs. (20) and (24) are used to calculate $A(t)$, it is found to be proportional to the temperature-dependent quantity τ_c^{-1}. In order to allow expression in terms of normalized variables alone, we introduce the new dimensionless quantity $A_1 \equiv \tau_{cn} A(t)$, which is still a function of both time and temperature. For simplicity, such dependence is explicitly suppressed, and A_1 is considered as a function of whatever variables are appropriate. Similarly, the explicit dependence of $\psi(t)$ or $\phi(t)$ on temperature and time is usually suppressed as well.

The previous equations now lead to

$$A_1 = (\mathrm{sgn}\gamma) BR^{-1} \times \begin{bmatrix} Y^{-(1+\rho_1)}\{\Gamma(1+\rho_1, Y) - \Gamma(1+\rho_1, bY)\} \\ + Y^{-(1+\rho_2)}\{\Gamma(1+\rho_2, aY) - \Gamma(1+\rho_2, Y)\} \end{bmatrix} u_0(Y), \tag{29}$$

$$\psi = u_0(Y) - (\mathrm{sgn}\gamma) B \times \begin{bmatrix} Y^{-\rho_1}\{\Gamma(\rho_1, Y) - \Gamma(\rho_1, bY)\} \\ + Y^{-\rho_2}\{\Gamma(\rho_2, aY) - \Gamma(\rho_2, Y)\} \end{bmatrix} u_0(Y). \tag{30}$$

Equations (29) and (30) are actually independent of the restrictive assumption $(ab)=1$ [or $\tau_c = (\tau_1\tau_2)^{\frac{1}{2}}$] which we generally employ herein. Note that $aY \equiv t/\tau_2$, $Y \equiv t/\tau_c$, and $bY \equiv t/\tau_1$. When $\beta_2 = 0$ and $\beta_1 \neq 0$, B, ρ_i, a, and b are all temperature independent, and the only remaining temperature dependence is that of R (which appears in Y as well as explicitly). When $Y \to 0+$, $A_1 \to A_{10}$, where A_{10} may be expressed as

$$A_{10} = R^{-1} \frac{[(1+\rho_1)^{-1}(b^{1+\rho_1} - 1) + (1+\rho_2)^{-1}(1 - a^{1+\rho_2})]}{[\rho_1^{-1}(b^{\rho_1} - 1) + \rho_2^{-1}(1 - a^{\rho_2})]}, \tag{31}$$

which becomes, when $\rho_1 = \rho_2 \equiv \rho$ and $ab = 1$,

$$A_{10} = R^{-1}\left[\frac{\rho}{1+\rho}\right] \frac{\sinh[(1+\rho)\sigma(\mathcal{E}_2 - \mathcal{E}_1)/2]}{\sinh[\xi(\mathcal{E}_2 - \mathcal{E}_1)/2]}, \tag{32}$$

for $\beta_2 \neq 0$. The temperature dependence of A_{10}, which is of considerable interest, is discussed in the next section. For the case $\beta_2 = 0$, $\beta_1 \neq 0$, the only temperature dependence of A_{10} enters through R since σ is replaced by 1 (except in R) and $\mathcal{E}$ by $\mathcal{L}$ in (32) in this case.

Since $\Gamma(1, Y) = \exp(-Y)$, Eqs. (29) and (30) simplify appreciably when $\rho_1 = \rho_2 = 0$ and when $\rho_1 = \rho_2 = 1$, respectively. For most cases of interest, there is an appreciable time interval over which one of the two terms within each set of curly brackets is negligible compared to the other and the other is virtually constant. Then only the $Y^{-(1+\rho_i)}$ term is of importance. For example, when $\gamma > 0$ and $\rho_1 = \rho_2 \equiv \rho$, $A_1 \cong BR^{-1}\Gamma(1+\rho) \times Y^{-(1+\rho)}$ for $aY \ll 1 \ll bY$ or $\tau_1 \ll t \ll \tau_2$. If further, $\rho = 0$, then $A_1 \cong BT^{-1} = [|\sigma|(\mathcal{E}_2 - \mathcal{E}_1)T]^{-1}$ in this time interval.

More generally, we may define T_1 as the normalized time at which A_1 begins to differ appreciably from A_{10}, T_c as the time at which a change of slope in a $\log A_1$ vs $\log T$ plot may be expected when $\rho_1 \neq \rho_2$, and T_2 as the time at which a final rapid drop-off of A_1 occurs. We may now somewhat arbitrarily determine T_1 and T_2 from the conditions $r^{|\sigma|}Y_1 = 1$, $r^{-|\sigma|}Y_2 = 1$, yielding $T_1 = Rr^{-|\sigma|}$, $T_2 = Rr^{|\sigma|}$, and $T_c = (T_1T_2)^{\frac{1}{2}} = R$ when $ab = 1$. Note that σ is set to unity here when $\beta_2 = 0$, $\beta_1 \neq 0$. When $\sigma = 0$, $A_1 = R^{-1}\exp(-Y)u_0(Y)$ and $T_1 = T_c = T_2 = R = \exp(-\sigma_n \mathcal{E}_c)$. It is clear from the definitions of a, b, and R that $t_1 = \tau_1, \tau_2$; $t_2 = \tau_2, \tau_1$ for $\sigma > 0$ and $\sigma < 0$, respectively. Thus, A_1 is virtually constant as long as t is less than the shortest relaxation time in the system, and it decreases towards zero very rapidly when t exceeds the longest relaxation time. When $\rho_2 = 0$, for example, the final decay is of the form $A_1 = B(t/\tau_{cn})^{-1} \times \exp(-t/t_2)$ for $t > t_2$.

Next, let us compare the transient responses of Eqs. (29) and (30) with those which follow from several other frequently used relaxation-time distributions. Transient response for the Cole–Cole distribution,[25] which involves the shape parameter m, cannot be expressed in closed form but leads to A_1 proportional to Y^{-m} for $Y \ll 1$ and to proportionality to $Y^{-(2-m)}$ for $Y \gg 1$. There is no final more rapid decay because the Cole–Cole distribution is nonzero in the entire range $0 < \tau < \infty$ and, therefore, $Y_1 = 0$, $Y_2 = \infty$. The present distribution can lead to a limited form of the above behavior when $\rho_2 = -\rho_1 = 1 - m$, yielding a distribution symmetrical in s. Then, A_1 is proportional to Y^{-m} for $Y \ll 1 \ll bY$ and to $Y^{-(2-m)}$ for $aY \ll 1 \ll Y$. For the Cole–Cole distribution, m is limited to $0 < m \leq 1$, but it is not so limited herein and has the temperature dependence implied by Eq. (27).[10]

The next distributions lead to results which may be compared to (29) and (30) in the special case $\rho_1 = \rho_2 = \rho$, which yields unsymmetrical distributions unless $\rho = 0$. First, the Davidson–Cole distribution,[4] which extends over a τ range from 0 to τ_c and involves the shape parameter $\beta (0 < \beta \leq 1)$, yields

$$A_1 = [R\Gamma(\beta)]^{-1} Y^{-(1-\beta)} e^{-Y} u_0(Y), \tag{33}$$

$$\psi = \{1 - [\Gamma(\beta, Y)/\Gamma(\beta)]\} u_0(Y). \tag{34}$$

When $Y \ll 1$, Eq. (33) leads to $Y^{-(1-\beta)}$ dependence, as does (29) over the range $aY \ll 1 \ll bY$ when $\rho = -\beta$. This correspondence holds only at a fixed temperature; note also that (33) yields the nonphysical result $A_1 \to \infty$ as $t \to 0$. The Cole–Cole and Cole–Davidson distributions

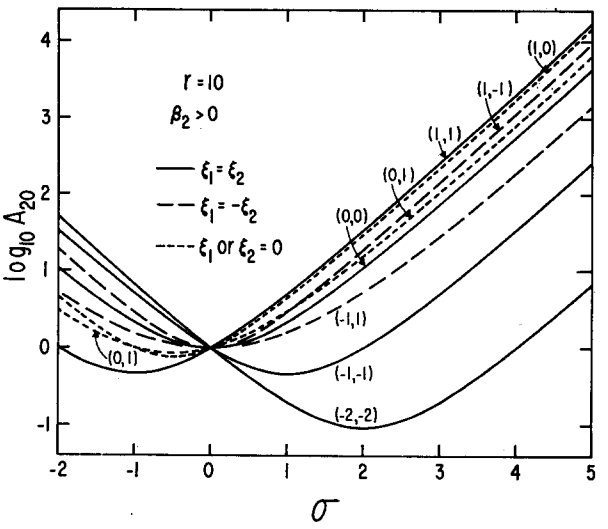

FIG. 1. The initial-time quantity $\log_{10}A_{20}=\log_{10}(RA_{10})$ vs the inverse temperature parameter σ for $r=10$ and various (ξ_1,ξ_2) values.

are both inconsistent[9] as well with a distribution of $\mathcal{E}$ and of $\mathcal{E}$ and $\mathcal{L}$.

Finally, let us consider the predictions of the truncated Karapetov–Voglis distribution.[8] We obtain from (20), (22), and (28), for $\gamma>0$,

$$A_1=[R\Gamma(-\nu,a)]^{-1}(1+Y)^{-(1-\nu)}\Gamma(1-\nu,a+aY)u_0(Y), \tag{35}$$

$$\psi=\{1-[\Gamma(-\nu,a+aY)/\Gamma(-\nu,a)](1+Y)^{\nu}\}u_0(Y). \tag{36}$$

In general, the quantity a must be replaced by $z_{\min}$. In the present case, $A_1\neq\infty$ at $t=0$, and $Y^{-(1-\nu)}$ response for A_1 is obtained in the interval $1\ll Y\ll a^{-1}$. Note that when $0\leq Y\ll a^{-1}$, the above expression for ψ is closely proportional[8] to $\ln(1+Y)$ for $\nu=0$ and to $\nu^{-1}[(1+Y)^{\nu}-1]$ for $|\nu|>0$.

VI. DISCUSSION OF CALCULATED RESULTS

Although tables of the incomplete gamma function $\Gamma(a,x)$ exist,[34] for the present work it has been found convenient to use a digital computer to calculate transient and temperature response from equations such as (28) and (29). Results of such calculation are discussed in the present section.

When the transient response of a linear system can be measured at times less than the shortest time constant or relaxation time of the system (excluding the "zero" time constant associated with ϵ_∞), A_1 approaches the constant value A_{10} as the time between the imposition of a forcing step function and the time of measurement decreases. Very few data of this type seem available, but measurements by Voglis[7] on current discharge from mica down to 10^{-2} sec after the beginning of discharge seem to indicate an approach to constancy. Voglis did not investigate temperature dependence, but other data on the discharge of two similar electrets at different temperatures[26] also show some tendency toward current constancy at short times after the beginning of discharge and indicate increased current at the higher temperature. Since the temperature dependence of the factor (C_s-C_∞) which enters into the current can usually be fitted by θ^{-n} dependence (with $n\approx1$) over an appreciable temperature range,[14,15] the electret data definitely indicate an increase in A_{10} with increasing temperature.

First, we are concerned with A_1 and ϕ time and temperature dependence when $\beta_2\neq0$ and there is more than one activation energy operative in the system. In Fig. 1, the quantity $\log_{10}A_{20}$ is plotted vs the normalized, shifted inverse temperature variable σ for various ξ_i values. Here $A_{20}\equiv RA_{10}$ is used instead of A_{10} in order to remove the temperature dependence of the R^{-1} term in A_{10} and so allow the appreciable differences between the results for different values of ξ_1 and ξ_2 to be clearly indicated. Note especially the reflection symmetry about the line $\sigma=0$ when $\xi_1=\xi_2\equiv\xi$ and the sign of ξ is changed. Also, when $\xi_1=\xi_2\equiv\xi$, the curves are symmetrical about the line $\sigma=-\xi$. The presence of the exponential dependence of R^{-1} on σ causes A_{10} to increase monotonically for all values of ξ_1 and ξ_2 as σ decreases and the temperature increases. This result is, therefore, in qualitative agreement with the electret data, but the actual temperature dependence of the theoretical A_{10} depends strongly on the values of such quantities as $\mathcal{E}_c$, ξ_i, and r.

There are a number of temperature-independent constants which must be chosen or determined when comparison is made between theoretical and experimental A_1 curves. A procedure for determining these quantities from transient response data is discussed below. A sufficient set of parameters is θ_n, τ_{cn}, σ_n, r, $\mathcal{E}_c$, ξ_1, and ξ_2. If theoretical A_1 curves are to be plotted in terms of normalized variables, only the last five parameters are required. Although we cannot hope to present herein curves which illustrate the effects of wide variations of all these parameters, we present representative cases which illustrate some of the general time-temperature behavior possible. For simplicity's sake, we hereafter take $\sigma_n=0$, since nonzero σ_n only causes equal translations of all curves on a log–log presentation. Note that the condition $\sigma_n=0$ implies the specific choice $\theta_n=\theta_\infty$.

Figures 2 and 3 show sets of curves for various values of ξ, and for $\mathcal{E}_1>0$, and $\mathcal{E}_1=0$. The case $\mathcal{E}_1=0$ is of special interest, even though it may only be approximated in physically realizable cases, because it leads, when $\sigma_n=0$, to $T_1=1$ for $\sigma>0$ and to $T_2=1$ when $\sigma<0$. In addition, when $\mathcal{E}_1=0$ and $\xi_1=\xi_2\equiv\xi$, A_{10} is proportional to σ^{-1} for $\sigma\mathcal{E}_2\gg1$.

The small solid dots on the curves of Figs. 2 and 3 show the positions of T_1 and T_2. Similarly, a larger circle is used to indicate T_c. Figure 2 shows curves for a very wide range of temperatures. In the special case

$\sigma_n=0$, e.g., $\sigma=-1$ implies $\theta=\infty$ and $\sigma=4$ requires $\theta=\theta_n/5$. When $\sigma_n<0$, however, σ may reach values appreciably more negative than -1 without necessitating $\theta=\infty$.

The condition $\sigma=0$, which implies $\theta=\theta_\infty>0$, is of particular importance because it leads to infinite values for ρ_i, to $G(\tau)=\delta(\tau-\tau_{c\infty})$, and to simple exponential decay for A_1 even though $\mathcal{L}$ and $\mathcal{E}$ may both be distributed. When $\sigma=0$, one also finds $T_1=T_c=T_2=1$, since $\tau_{cn}=\tau_{c\infty}$ for the present choice of $\sigma_n=0$.

Figures 2 and 3 show that as σ decreases, T_2 always decreases (when $\mathcal{E}_1>0$) and A_{10} always increases. This behavior is a consequence of the normalization condition. Since $\psi(\infty)=1$, the total area under the A_1 vs T curve must always be unity, independent of σ.

Comparison of the $\sigma=\pm1$ curves of Fig. 2(a) with

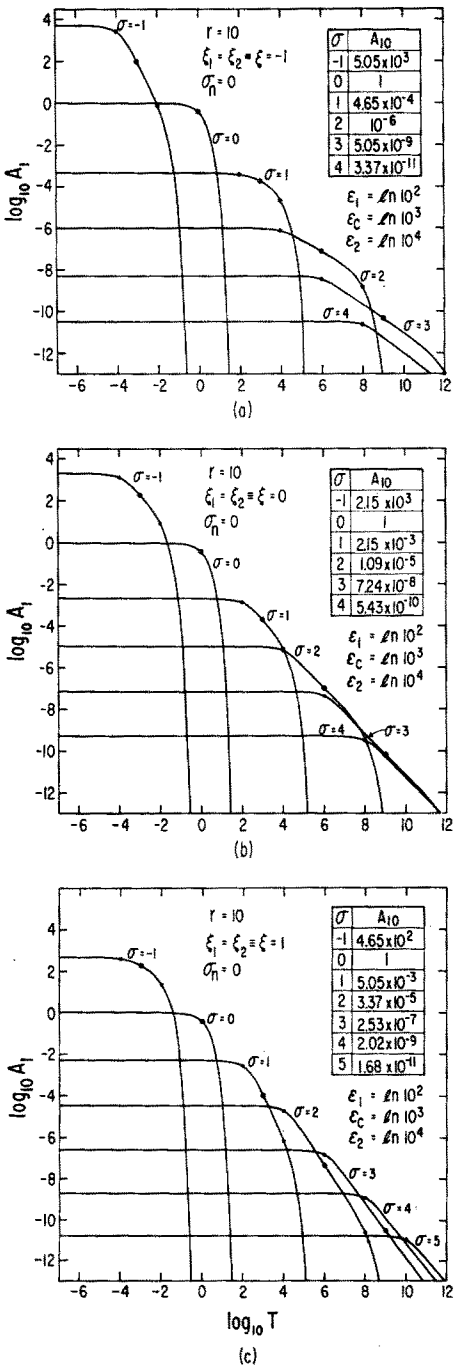

FIG. 2. The normalized transient response function A_1 vs normalized time T for several ξ and σ values (log–log presentation).

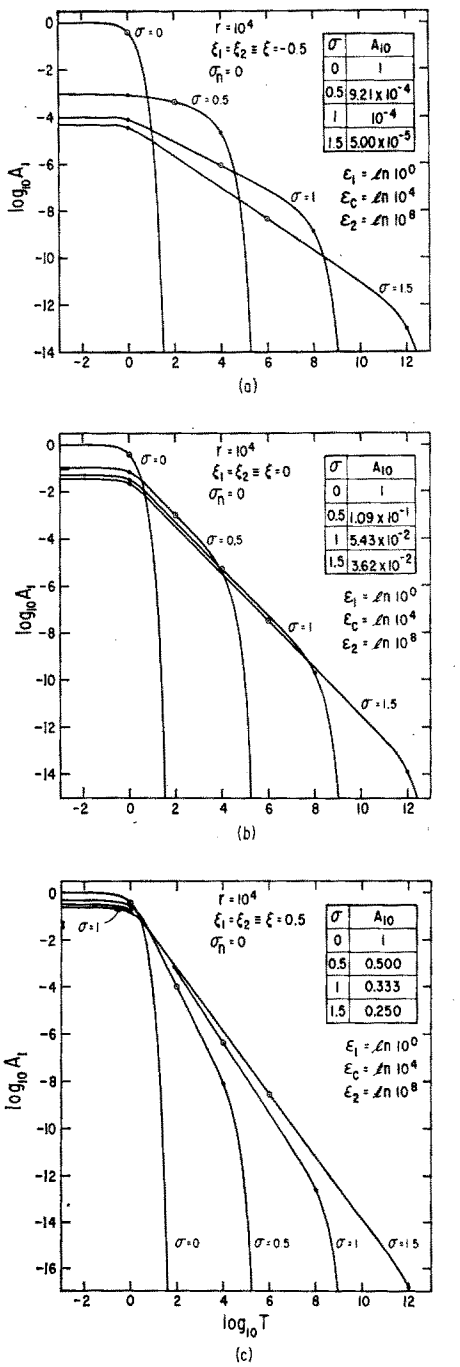

FIG. 3. The normalized transient response function A_1 vs normalized time T for several ξ and σ values (log–log presentation).

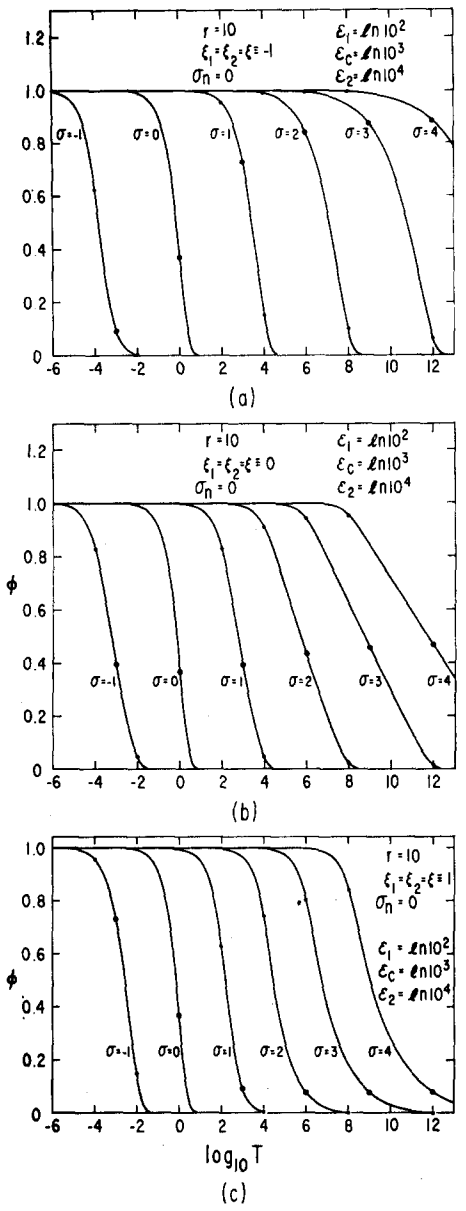

FIG 4. The relaxation function ϕ vs normalized time T for several ξ and σ values (semilog presentation).

the $\sigma=\mp 1$ curves of Fig. 2(c), respectively, shows that corresponding curves are the same except for horizontal and vertical translations of six decades. The translations arise from the different values of R appropriate to the two σ values, while the equality of shape follows from the equal values of $|\sigma|$ and of $\rho_1=\rho_2=\rho$ for the two curves compared. Thus, curves calculated for a given ξ can also be used, after translation, for those with $-\xi$.

Since the range $(T_2/T_1)=r^{2|\sigma|}$ increases as $|\sigma|$ increases, the curves show a wider and wider region of constant slope, equal to $-(1+\rho)$, as $|\sigma|$ increases. But since $\rho=\xi/\sigma$ here, the slope of the straight-line portion approaches -1 in the limit of large $|\sigma|$. Note that the signs of both σ and ξ determine whether the final slope is approached from below or above. The present $T^{-(1+\rho)}$ behavior has been widely found for a variety of situations.[7,24–28,37] The quantity ρ is almost always in the range $-0.5\leq\rho\leq 0.5$ and is usually found in the range $-0.2\leq\rho\leq 0.2$. The present results suggest a reason why it is usually relatively small. Whenever a thermally activated process is present and $\beta_2\neq 0$, the range over which $T^{-(1+\rho)}$ behavior can appear increases as $|\sigma|$ increases. Thus, it may happen that a $|\sigma|$ large enough to yield an appreciable $T^{-(1+\rho)}$ range is also large enough to cause $|\rho|=|\xi/\sigma|$ to be small.

An idea of the range of $|\rho_i|$ may be obtained from the physics of the situation. For simplicity, take $\beta_1=0$ and $\mathcal{S}\equiv E$. Then, since E obeys an exponential type of distribution, $|\lambda_i|^{-1}$ may be roughly interpreted as the mean activation energy for transition from one state to another for the τ range over which λ_i is the applicable parameter. This energy is likely to be of the order of $k\theta_0$ or less in cases of experimental interest. But in the present situation $|\rho_i|=|\lambda_i k\theta_0/[(\theta_0/\theta)-1]|$, since β_2^{-1} equals $k\theta_n$. Since θ is always appreciably less than θ_0, we find that $|\rho_i|\approx(\theta/\theta_0)$ when $|\lambda_i^{-1}|\approx k\theta_0$ in the present case. Also, when both β_1 and β_2 are nonzero and β_1/β_2 negative, although it may be possible to decrease σ sufficiently to cause $|\rho_i|$ to exceed unity by an appreciable factor, the concomitant decrease in the range T_2/T_1 will lead to elimination of any region of $T^{-(1+\rho)}$ dependence. Thus, in both cases, one does not expect to find $T^{-(1+\rho)}$ dependence with $|\rho|\geq 1$. Unfortunately, little transient or frequency response measurements seem yet available over a wide enough range of temperatures to allow the dependence of ρ on temperature to be accurately determined. What data are available, however, seem to suggest either a temperature-independent $\rho(\beta_2=0)$ or temperature dependence in rough agreement with the predictions of the present work when $\beta_2\neq 0$.[9,10,11,32]

Since $\sigma=[\theta_n/\theta)-(\theta_n/\theta_\infty)]$, σ can only go negative if (θ_n/θ_∞) is positive. But because θ is usually experimentally limited to values below θ_0, σ does not become zero or negative unless $(\beta_1/\beta_2)<0$, requiring positive correlation between $\mathcal{S}$ and $\ln(\nu_d/\nu_{dc})$. If (β_1/β_2) is sufficiently negative, the measuring temperature may be varied over a wide enough range that $T^{-(1+\rho)}$ behavior is noted for both $\sigma>0$ and $\sigma<0$; the sign of ρ is different in these two regions as well, of course. Alternatively, when $(\beta_1/\beta_2)>0$, the minimum experimentally achievable value of σ will be positive and may be sufficiently large that $T^{-(1+\rho)}$ behavior still remains at the highest possible measuring temperature.

Figure 3 with $\mathcal{E}_1=0$ shows results when r is larger than that of Fig. 2 but the temperature range is smaller. Here the larger r value leads to a greater increase in the range (T_2/T_1) for a smaller temperature change than is required for the case of Fig. 2. At the point $\log_{10}T\simeq 0.75$

[37] M. F. Manning and M. E. Bell, Revs. Mod. Phys. 12, 215 (1940).

of Fig. 3(c) where several of the curves nearly cross, there is virtually no temperature dependence of A_1 over the entire range $0.5 \leq \sigma \leq 1.5$.

Figures 4 and 5 show the ϕ curves corresponding to the A_1 cases of Figs. 2 and 3, respectively. Here, however, a linear scale for ϕ is used. These curves can represent the decay of charge during the discharge of a fully charged capacitor or the relaxation of stress after the application of a step function of strain at $t=0$ to a mechanical system. Alternatively, if the present ϕ curves are rotated 180° about the line $\phi=1$ and unity subtracted from the result, one obtains, for $t>0$, $\psi=1-\phi$. The ψ curves then represent the charge during step-function charging of a capacitor or the strain after the application of a step function of stress.

Figure 4 shows that for any value of ξ the shape of the decay curves changes appreciably as σ increases. For $\xi=0$ the change is a progressive decrease in the slope of the decay lines while for $\xi<0$ and $\xi>0$ the decreases in decay rate primarily occur near $\phi \lesssim 1$ and $\phi \gtrsim 0$, respectively. For $\xi=0$, the $\sigma=-1$ and $\sigma=+1$ curves are of exactly the same shape, but this is not the case when $\xi \neq 0$. Particularly noteworthy is the way the positions of T_1, T_c, and T_2 fall on the curves (indicated by the solid dots) as σ or ξ is varied.

The curves of Fig. 5 are of the same general shape as the corresponding ones of Fig. 4 but the choice $\mathcal{E}_1=0$ of course causes T_1 to be unity, independent of σ for all curves. This effect of constant T_1 is obviously particularly pronounced for the $\xi>0$ curves of Fig. 5(c). When $\xi=0$, the $\sigma=2$ curve of Fig. 4 is identical in shape with the $\sigma=0.5$ curve of Fig. 5, as are the corresponding $\sigma=4$ and $\sigma=1$ curves. This is because r^σ is the same for these choices, causing the range T_2/T_1 to be the same. A different comparison is appropriate when $\xi \neq 0$. For example, the curves for $\xi=-1$, $\sigma=1$ of Fig. 4 and $\xi=-0.5$, $\sigma=0.5$ of Fig. 5 are nearly the same in shape because these choices cause the corresponding ρ's to be the same. The appreciable difference in range between the two curves shows up only in a relatively small difference in the shape of the curves for $0.8<\phi \leq 1$. For $\xi>0$, curves of Figs. 4 and 5 having the same ρ are virtually the same in shape except in the region $0 \leq \phi < 0.2$.

Although the majority of ϕ and ψ curves for mechanical systems seem to change their shape only slightly if at all when the temperature of measurement is changed within a limited range, this is not always the case. Stress relaxation results on polysulfide rubbers[38,39] and creep recovery results on rosin, phenolphthalein, and soft and hard rubber by Kobeko *et al.*[33] show definite change of curve shape with temperature in qualitative agreement with some of the results of Figs. 4 and 5.

All of the curves of Figs. 2 through 5 are also pertinent in the case $\beta_2=0$, $\beta_1 \neq 0$, where $\mathcal{L}$ alone is distributed,

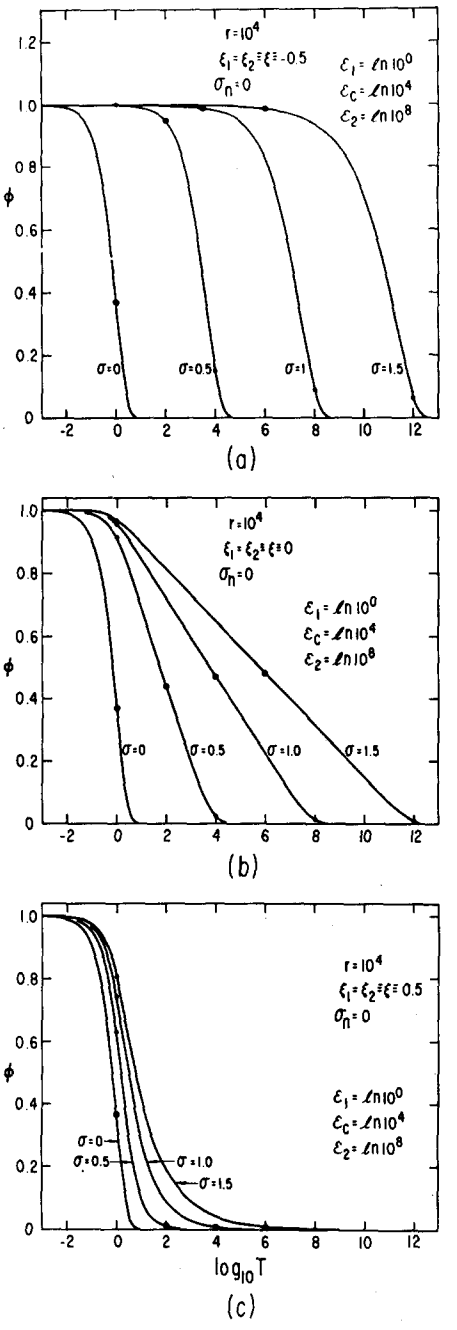

FIG. 5. The relaxation function ϕ vs normalized time T for several ξ and σ values (semilog presentation).

provided the proper temperature-independent range and ρ values are taken. If the single $\mathcal{E}$ value present in the $\beta_2=0$ case is taken as $\mathcal{E}_c$ and given the same value as in the $\beta_2 \neq 0$ situation, then R and its temperature dependence will be the same in the two cases and no translation on the log–log plot will be necessary in going from one case to the other. In transforming from the $\beta_2 \neq 0$ case to that where $\beta_2=0$, all σ values in formulas are to be replaced by unity except the quantity $(\sigma-\sigma_n)$ which appears in R; this is equal to $(\eta-\eta_n)=(\theta_n/\theta)-1$.

[38] M. D. Stern and A. V. Tobolsky, J. Chem. Phys. **14**, 93 (1946).
[39] P. Feltham, Brit. J. Appl. Phys. **6**, 26 (1955).

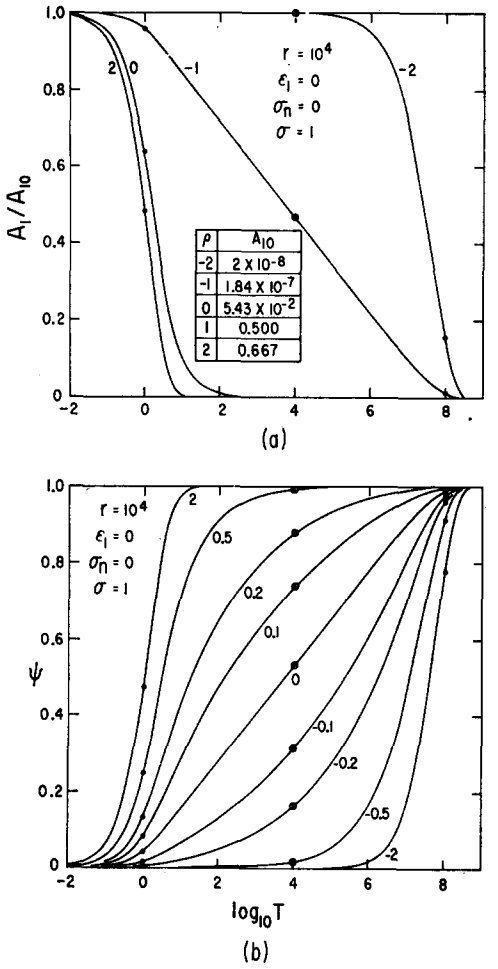

FIG. 6. The quantities A_1/A_{10} and ψ vs $\log_{10} T$ for $\sigma=1$ and various ρ values.

Thus, in the present case of $\sigma_n=0$, the quantity σ, taken as a measure of temperature on the curves of Figs. 2 and 3, may be interpreted as $(\theta_n/\theta)-1$ whether $\beta_2\neq 0$ or $\beta_2=0$.

As examples, the $\sigma=0$ curve of Fig. 3(a) is applicable when $\beta_2=0$ provided $\theta=\theta_n$ and $r=1$; a case where $\mathcal{L}$ is not distributed. The $\sigma=0.5$ curve of this figure is appropriate when $\theta=2\theta_n/3$ for $r=10^2$ and $\rho=\xi=-1$, etc. Note that in the present case, since the range and ρ are temperature independent, the shape of a given curve remains invariant as θ changes and such change only produces horizontal and vertical translations on a log–log plot, arising from the temperature dependence of R. In the present situation of $\beta_2=0$ and $\rho_1=\rho_2=\rho=\xi$, the only temperature dependence of A_1 in the region of $T^{-(1+\rho)}$ behavior arises from a factor $R^\rho=\exp[\{(\theta_n/\theta)-1\}\xi\mathcal{E}_c]$, which may either lead to a decrease or increase with increasing temperature, depending on the sign of ξ.

In the case $\beta_2=0$, the quantities ϕ, ψ, and RA_1 obey a time-temperature superposition law (the TTS law) such as that widely applied in transient and frequency response analysis of polymers.[15,40,41] The only temperature dependence of ϕ, ψ, and $RA_1=\tau_c A(t)$ appears in the variable Y and so only in the time-temperature combination $TR^{-1}=T\exp[-\{(\theta_n/\theta)-1\}\mathcal{E}_c]=t\tau_{dc}^{-1}\exp[-\{(\theta_n/\theta)-(\theta_n/\theta_0)\}\mathcal{E}_c]$. Thus, temperature change produces shifts but no change in curve shape. Therefore, the effect of an increase of the temperature-independent time variable T could as well be produced by an increase in θ, and when $\beta_2=0$, ψ, and ϕ curves may be considered as functions of $[1-\theta_n/\theta]$ instead of $\log_{10}T$. The situation where $\mathcal{L}$ alone is distributed is plausible for amorphous polymers because their response to a mechanical stimulus involves a large number of polymer chain segments of varying length. Thus, each different segment has a different natural frequency of vibration but is, on the average surrounded by a similar intermolecular force field, leading to a single or narrowly distributed activation energy.[15,30,40,42]

The TTS law has been found to apply quite well for a variety of nonpolar substances.[40] On the other hand, when the material involves polar forces, it is not to be expected that all elements involved in its response will find themselves in equivalent surroundings. Then, one may expect that $\mathcal{E}$ or $\mathcal{E}$ and $\mathcal{L}$ may be distributed. In these cases, which might be pertinent for both the mechanical and electrical response of polar substances, of solid mixtures[15] ($\mathcal{E}$ alone distributed), or of partially crystalline polymers[15] ($\mathcal{E}$ and $\mathcal{L}$ distributed), one would not expect the TTS law to apply.

Before discussing further calculated curves, it may be useful to show how pertinent parameters may be derived from a comparison of theoretical and experimental curves. In making such comparison, which we confine to the A_1 level, it is frequently unnecessary to calculate the exact form of theoretical curves using values of $\Gamma(a,x)$; instead, it is usually sufficient to approximate a theoretical log–log curve by first a horizontal portion ending at $T=T_1$; then a straight line of $-(1+\rho_1)$ slope until $T=T_c$; next a straight line of $-(1+\rho_2)$ slope up to $T=T_2$; and finally a rapid drop-off for $T>T_2$. The present results may then be used for the dependence of A_{10}, ρ_1, and ρ_2 on temperature. This method of approximation is clearly inapplicable when no $T^{-(1+\rho)}$ straight-line region occurs, e.g., because the range is too small.

For simplicity, we discuss theoretical–experimental comparison principally for the case $\beta_2\neq 0$, $\rho_1=\rho_2=\rho$, and $ab=1$. It is assumed that transient measurements are available for at least two different temperatures and cover a sufficient time span that t_1 and t_2 can be established at each temperature. Consideration of temperature dependence of A_1 immediately establishes whether $\sigma>0$ or $\sigma<0$. Then the t_1 and t_2 values at a given tem-

[40] A. J. Staverman and F. Schwarzl, *Die Physik der Hochpolymer*, edited by H. A. Stuart (Springer-Verlag, Berlin, 1956), Vol. 4, pp. 56–62.
[41] See reference 30, p. 144 ff.
[42] O. Nakada, J. Phys. Soc. Japan **12**, 1218 (1957).

perature, say θ_n, yield τ_{1n}, τ_{2n}, and τ_{cn}. Further measurements at $\theta=\theta_j\neq\theta_n$ yield τ_{1j}, τ_{2j}, and τ_{cj}, leading to the value of $R=\tau_{cj}/\tau_{cn}$ appropriate at θ_j. From this value of R, the quantity $\mathcal{E}_c$ may then be calculated. Next, T_1, T_2, T_c, a, and b can be calculated for the two temperatures. The quantity $\ln(T_2/T_1)$ at the two temperatures may then be used to yield σ_n and r, and finally σ_j. From r and $\mathcal{E}_c$, one can then calculate $\mathcal{E}_1$ and $\mathcal{E}_2$. Then, knowledge of $(\rho)_n$ or $(\rho)_j$ allows ξ to be obtained. If the quantity θ_0 can be estimated theoretically or obtained experimentally from another kind of measurement, then (β_1/β_2) can be calculated using σ_n. Note that $(\mathcal{L}_2-\mathcal{L}_1)=(\beta_1/\beta_2)(\mathcal{E}_2-\mathcal{E}_1)$, allowing $(\mathcal{L}_2-\mathcal{L}_1)=\ln(\tau_{d2}/\tau_{d1})$ to be obtained. Without further information, such as knowledge of λ, it does not seem possible to get β_1 and β_2 separately, although if β_2 is taken positive, the sign of β_1 is fixed. Note that when $\beta_2=0$ and $\beta_1\neq0$, ρ may be obtained at any temperature and is equal to $\xi=\lambda/\beta_1$. Again, β_1 cannot be obtained without further knowledge of the theoretical relationship between $\mathcal{S}$ and $\mathcal{L}$.

Figure 6(a) shows (A_1/A_{10}) vs $\log_{10}T$ for fixed temperature and several values of ρ. When $\rho=-1$, A_1 shows a considerable straight-line region and A_1/A_{10} may be quite well approximated over most of the range of T shown by $[1-a_1\ln(1+b_1T)]$, where a_1 and b_1 are constants. The $\rho=-1$ curve may also be approximated by straight-line segments.[43] Figure 6(b) presents similar curves for ψ. Comparison of Figs. 6(a) and 6(b) shows that the A_1/A_{10} curve for $\rho=-1$ is identical with the $\phi\equiv u_0(t)-\psi$ curve for $\rho=0$. This result follows from the present special form of $G(\tau)$ in Eq. (24). For such power-law dependence, in fact, the more general result holds that for all finite ρ_i values, $(A_1/A_{10})_{\rho_1,\rho_2}=(\phi)_{1+\rho_1,1+\rho_2}$, as may be directly verified from Eqs. (29)–(31). Thus, all the ϕ and ψ curves of Figs. 4, 5, and 6(b) may be carried over to A_1/A_{10} curves, such as those in Fig. 6(a), by letting $\rho_i\rightarrow\rho_i-1$. Further, all the present constant-temperature log–logA_1 curves of the present paper may be considered as log–logϕ curves with ρ_i values increased by unity provided the curves are translated vertically by an amount sufficient to make $A_{10}=1$. Note that in agreement with Table I as $|\rho|$ increases and thus as $\rho\rightarrow\pm\infty$, A_1/A_{10} or ϕ approaches $\exp(-T/T_i)$, where $T_i=T_1$ for $+\infty$ and $T_i=T_2$ for $-\infty$. For $\rho_1\rightarrow\infty$, $\rho_2\rightarrow-\infty$, the corresponding result for ϕ would be $[\exp(-T/T_1)+\exp(-T/T_2)]/2$.

The results of many creep retardation experiments and many mechanical stress relaxation experiments may be described over an appreciable span of time by either $\psi\simeq a_1\ln(1+b_1t)u_0(t)$ or the corresponding $\phi=u_0(t)-\psi$ expression, respectively, where b_1 is a constant.[8,44] Such dependence, or simpler ln$t$ dependence, has, in fact, been found in a wide variety of situations, including aging of barium titanate,[45] magnetic viscosity,[46] and chemisorption and oxidation.[47] It is, however, sometimes associated with nonlinear rather than linear behavior. Whenever dielectric charging or discharge experiments show t^{-1} current behavior over an appreciable time range, probably the most common behavior next to simple exponential decay, the charge on charging from an uncharged condition will also exhibit $\ln(b_1t)$ response over part of the charging curve. Since the ψ curve for $\rho=0$ in Fig. 6(b) can be well approximated by behavior

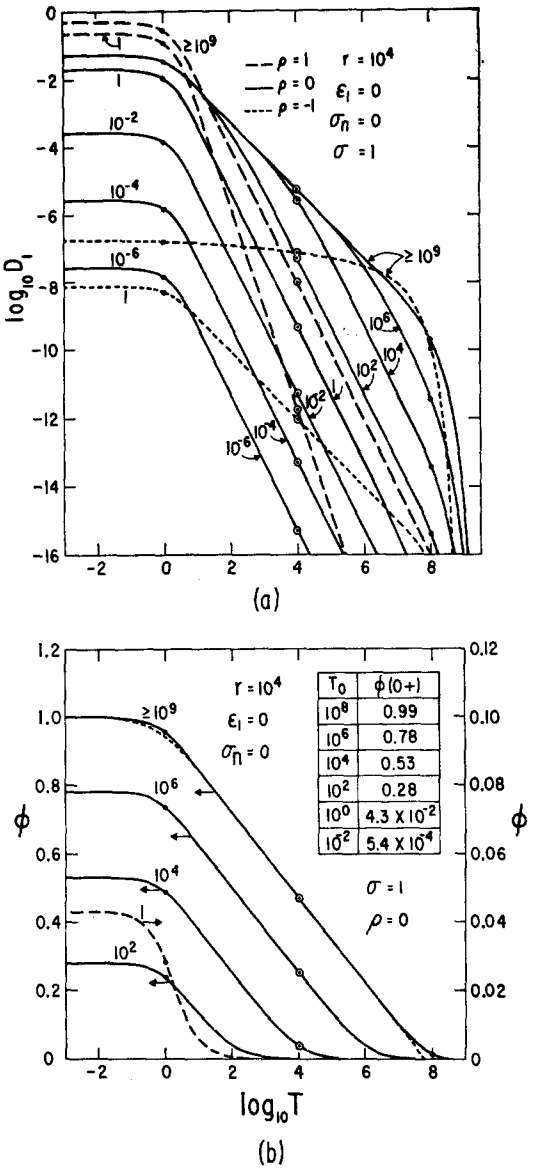

FIG. 7. The quantities $\log_{10}D_1$ and ϕ vs $\log_{10}T$ for $\sigma=1$ and various T_0 values. Here ϕ gives the normalized charge remaining in the system after charging from a zero-charge state for a time T_0, then discharging at $T=0$. $D_1=-d\phi/dT$.

[43] See reference 30, pp. 125–126.

[44] D. Kuhlmann, Z. Physik **124**, 468 (1947).

[45] M. C. McQuarrie and W. R. Buessem, Bull. Am. Ceram. Soc. **34**, 402 (1955).

[46] R. Street and J. C. Wooley, Proc. Phys. Soc. (London) **A62**, 562 (1949).

[47] P. T. Landsberg, J. Appl. Phys. **33**, 2251 (1962).

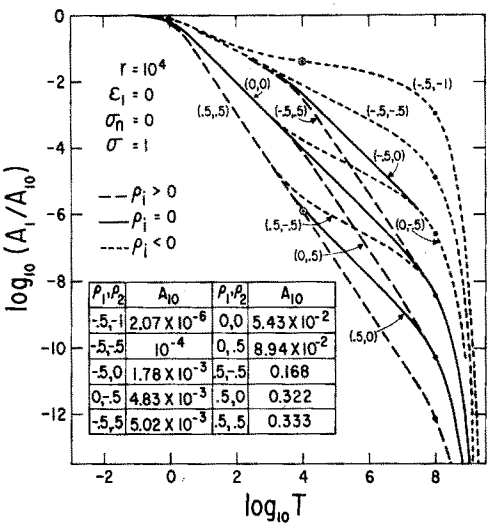

FIG. 8. Curves designated by (ρ_1,ρ_2) values showing the effect on $\log_{10}(A_1/A_{10})$ of different ρ_1 and ρ_2 values for $\sigma=1$.

of this type over most of the pertinent T range, the present distribution with $\rho_1=\rho_2=0$ may be used to describe such creep or dielectric data and is preferable to alternative approximation using the K–V distribution for reasons already discussed.

It should be noted in Fig. 6(b) that $|\rho|$ values even as large as 0.1 lead to appreciable curve portions which might be mistaken for $\ln(b_1 t)$ dependence. Thus, in determining ρ from ψ data for which experimental error is not negligible, it is clearly desirable to have available data covering as wide a time span as possible. As might be expected, an increase in r from 10^4 to 10^8 produces a completely negligible change in, for example, the $\rho=0.5$ curve of Fig. 6(b). On the other hand, such a change, since it affects T_c and T_2, leads to a very important change in the $\rho=-0.5$ curve, for example. It remains of very nearly the present form but is translated eight decades to the right.

Figure 7 shows discharging curves after noninfinite charging times. Here D_1 is normalized similarly to A_1 and is, from Eq. (9), $[A_1(T)-A_1(T+T_0)u_0(T)]$, where $T_0\equiv t_0/\tau_{cn}$ and t_0 is the charging time before the beginning of discharge at $T=0$. The parameter shown on the various curves is T_0, and it is clear that T_0 must exceed T_2 (t_0 must exceed the longest time constant in the system) before the discharge curve approximates well to that for infinite prior charging from a zero charge condition. The necessity for such long charging is frequently overlooked. Voglis[7] has purposely discharged mica samples after varying charging times and found current curves of the same general character as those for $\rho=0$ in Fig. 7(a) but, in his case, the best value of ρ is about -0.13. His charging times roughly cover the range equivalent to $T_0=10^2$ to $T_0\geq 10^9$ of the present figure. It is worth mentioning that the present curves for $T_0<T_2$ and those of Voglis differ appreciably in form from curves calculated for a similar situation from a Gaussian RTDF[11] with $0<\tau<\infty$.

Also shown in Fig. 7(a) are curves for $\rho=1$ and -1 for $T_0\geq 10^9$ and $T_0=1$. It is noted that when $T_0\ll T_2$, the straight-line slope of the curves, when it appears, is not $T^{-(1+\rho)}$ as it is for $T_0\geq T_2$ but is $T^{-(2+\rho)}$. This follows because series expansion of D_1 shows that for $T_0\ll T$, D_1 is closely equal to $-T_0(dA_1/dT)$. This derivative has also been separately calculated in the computer program. Since it approaches a constant as $T\rightarrow 0$, D_{10} becomes proportional to T_0 for $T_0\ll T_1$. The resulting decrease of D_{10} below the value appropriate for $T_0=\infty$ shows that when $T_0\leq T_1$ the charging time is insufficient to charge fully even the element of the system having the shortest relaxation time.

In Fig. 7(b), the normalized charge remaining in the system after charging for a time T_0 and discharging for a time T, $\phi(T)\equiv\psi(T+T_0)u_0(T)-\psi(T)$, is plotted vs $\log_{10}T$ for several T_0 values. In this case of finite charging, $\phi(T)$ is given by the integral of $D_1(T)$ from 0 to ∞ minus that from 0 to T. When $T_0\rightarrow\infty$ and $T>0$, this definition yields the usual $1-\psi$ for ϕ. The table in Fig. 5(b) shows $\phi(0+)=\psi(T_0)$, the relative proportion of full charge in the system at the instant of discharge. In the limit $T_0\rightarrow 0$, $\phi(T)\rightarrow T_0A_1(T)$, so that $\phi(0+)$ approaches T_0A_{10}. These results again emphasize the necessity for T_0 to exceed T_2 if the complete discharge curve is desired. Only when $T_0\gg T_2$ should a discharge current curve be compared with the charging current obtained starting from zero initial charge.

The dashed curve in Fig. 7(b) has been plotted with an expanded scale as indicated by the arrow. The dotted curve shows the fit obtained to the infinite-charging-time ϕ curve by an expression of the form $[1-a_1\ln(1+b_1T)]$. The solid curve marked $\geq 10^9$ is identical in form with the $\rho=-1$ curve of Fig. 6(a), as mentioned previously. It is not quite symmetrical about $T=T_c$ but approaches such symmetry as T_2/T_1 increases.

Figure 8 is included to show the effect of various combinations of ρ_1 and ρ_2 on the shape of the current transient response. It is clear that the slope of the line in the interval $T_1<T<T_c$ is $-(1+\rho_1)$ while that appearing in $T_c<T<T_2$ is $-(1+\rho_2)$. Note that unless measurements are extended considerably beyond $T=T_2$, the increased decay rate at $T\geq T_c$ arising from ρ_2 in the case $\rho_2>\rho_1$ may be mistaken for the final decay appearing at $T\geq T_2$. Decays in these two regions may be distinguished even when T cannot be extended to T_2 because $-(1+\rho_2)$ decay yields a straight line on a log–log plot while decay when T exceeds the longest time constant of the system leads to a curve with continually increasing slope magnitude. Finally, care should be exercised that an increased decay rate in the region $T_1<T<T_2$ does not arise from too short charging, as exemplified by the $T_0=10^4$ curve of Fig. 7(a).

The $(-0.5,-1)$ curve of Fig. 8 has a portion between $\log_{10}T=3.5$ and 6.5 arising from the choice $\rho_2=-1$,

where A_1 decreases almost linearly with $\log_{10}T$. Such linear behavior is characteristic of the wedge-box distribution over part of the pertinent time range. Values of (ρ_1,ρ_2) of (0.5, 0) are usually chosen, however, for wedge-box behavior, which makes such behavior appear in ϕ rather than A_1 as it does here. Then, the resulting ϕ is used to describe the relaxation of stress under constant strain. As already mentioned, there is, however, no real distinction between constant-temperature log–logA_1 and ϕ time curves of the present paper provided ρ_i values are suitably transformed.

Stress relaxation curves at constant strain for polymers frequently exhibit[30] transient behavior in which $\rho_1>\rho_2$, as in the restrictive case of the wedge-box distribution. On the other hand, considerable retardation dielectric data on a variety of materials shows $\rho_1=\rho_2$ behavior over the range of times investigated. Finally, some organic and inorganic materials such as wax electrets,[26] amber,[25] kerafar U,[7] petroleum,[24] rutile,[28] and Teflon[27] seem to show some tendency for ρ_1 to be less than ρ_2 for the dielectric retardation situation. No presently available data on such materials extend to long enough times to allow the final $T>T_2$ decay region to be unambiguously identified. Note that this region may be made to occur at shorter times by raising the temperature, but if $\mathcal{E}$ is distributed, the range T_2/T_1 may be too much reduced thereby to allow ρ_1 and ρ_2 to be determined. It would be particularly valuable, however, for dielectric transient response curves to be obtained which include shorter times after the start of discharge, extend to longer decay times, and cover a wider range of temperature than any currently available.

One reason for the above trend for ρ_1 to exceed ρ_2 in stress relaxation situations and for ρ_1 to be equal to or less than ρ_2 for retardation is that for the same material there is some tendency for the distribution function $F(\tau)\equiv\tau G(\tau)$ for relaxation to be the approximate inverse of that for retardation. For the present form of $G(\tau)$, such inversion of $F(\tau)$ is equivalent to the transformation from ρ_i to $-\rho_i$. For a choice of $\rho=0.5$ for relaxation (the wedge distribution) Smith[48] has shown that when T_2/T_1 is appreciable, the corresponding $G(\tau)$ [or $F(\tau)$] for retardation is of very nearly the form of (24) with $\rho=-0.5$ over most of the pertinent range. It is the above property of invariance of the form of the present expression for $F(\tau)$ under inversion which makes it and the corresponding $G(\tau)$ of particular value as distribution functions useful for both retardation and relaxation situations.

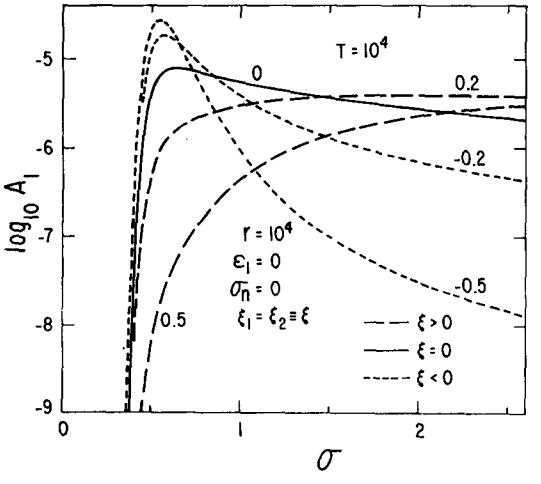

FIG. 9. Dependence of $\log_{10}A_1$ on the inverse temperature variable σ for $T=10^4$ and several $\xi_1=\xi_2=\xi$ values. $(\beta_2>0)$.

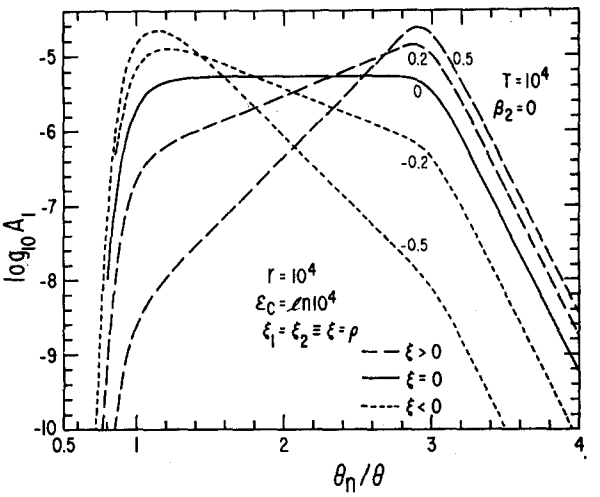

FIG. 10. Dependence of $\log_{10}A_1$ on the inverse temperature variable (θ_n/θ) for $T=10^4$ and several $\xi_1=\xi_2=\xi=\rho$ values $(\beta_2=0, \beta_1\neq 0)$.

Considerable idea of the temperature response of current at a fixed $T>T_1$ may be obtained by comparison of the various σ curves of Figs. 2 and 3 at fixed T. More directly, Fig. 9 shows expected temperature dependence of $\log_{10}A_1$ at $T=10^4$ for five different ξ values in the case $\beta_2\neq 0$. Logarithmic current curves qualitatively similar to that for $\xi=0$ have been found for fluorothene and Lucite by Munick[27] at $t=100$ sec after the beginning of charging or discharge. The apparent value of ρ for these polar materials is very nearly zero. Measurements were extended over the range from about $-180°$ to 47°C.

Figure 10 shows similar theoretical curves for the case $\beta_2=0$. Since only $\mathcal{E}$ or $-\mathcal{E}$ is distributed here, the temperature variable σ has been replaced by θ_n/θ for this case. Note that although θ_n is arbitrary, the fixed value of $T=t/\tau_{cn}=10^4$ involves it through τ_{cn}. The $\rho=0$ curve in Fig. 10 is not quite as similar to Munick's experimental results as is that in Fig. 9. The primary differences between curves of Figs. 9 and 10 occur because neither ρ_i nor the range is temperature dependent when $\beta_2=0$. The decreases at both ends of the curves of Fig. 10 occur, however, because T_1 and T_2 do still depend on temperature through R.

In order to show the temperature dependence of stress relaxation at constant time after the imposition

[48] T. L. Smith, Trans. Soc. Rheol. 2, 131 (1958).

of strain, one must consider the quantity ϕ. Figure 11 shows the quantity $\log_{10}\phi$ vs either θ_n/θ or $(\sigma+1)$, depending on whether $\beta_2=0$ or $\beta_2\neq 0$, respectively. Again, the value $T=10^4$ is selected. Only one ϕ curve for the case $\beta_2=0$ has been included in Fig. 11 because the system then obeys the time–temperature superposition law and earlier ϕ or A_1/A_{10} curves for fixed θ and variable T may readily be interpreted as curves for fixed T and variable θ. Specifically, let us denote the fixed T value used with variable θ as T_m and the fixed θ value used with variable T as θ_m. Then, when the TTS law holds, it follows that the $\log_{10}T$ and θ_n/θ scales are related by $\log_{10}T+(\mathcal{E}_c\log_{10}e)(\theta_n/\theta)=\log T_m+(\mathcal{E}_c\log_{10}e)(\theta_n/\theta_m)$. In much of the present work, we have taken $\log_{10}T_m=4$, $\mathcal{E}_c\log_{10}e=4$, and $\sigma_m=1$, where the latter value corresponds in the present case of $\sigma_n=0$ to $(\theta_n/\theta_m)=2$. Thus, the two possible scales are here related by $\log_{10}T+4(\theta_n/\theta)=12$. All the foregoing ϕ and A_1/A_{10} curves plotted vs $\log_{10}T$ may thus be considered as alternatively plotted vs $(\theta_n/\theta)=(12-\log_{10}T)/4$. The present $\xi_1=0.5$, $\xi_2=0$ curve of Fig. 11 for $\beta_2=0$ is thus, in fact, of exactly the same shape (after reflection in the (θ_n/θ) axis) as the $\xi_1=-0.5$, $\xi_2=-1$ curve of Fig. 8. When shape alone is important, all the present $\sigma=1$, $\log_{10}A_1$ curves plotted vs $\log_{10}T$ may be considered as $\log_{10}\phi$ curves vs (θ_n/θ) in the case $\beta_2=0$ provided ξ_i values are transformed as well. It is important to note, however, that the $\log_{10}A_1$ curves of Fig. 10 plotted vs (θ_n/θ) cannot be transformed directly to $\log_{10}\phi$ curves vs $\log_{10}T$ because ϕ is related to A_1/A_{10} not just to A_1, and although A_{10} is time invariant, it is temperature dependent.

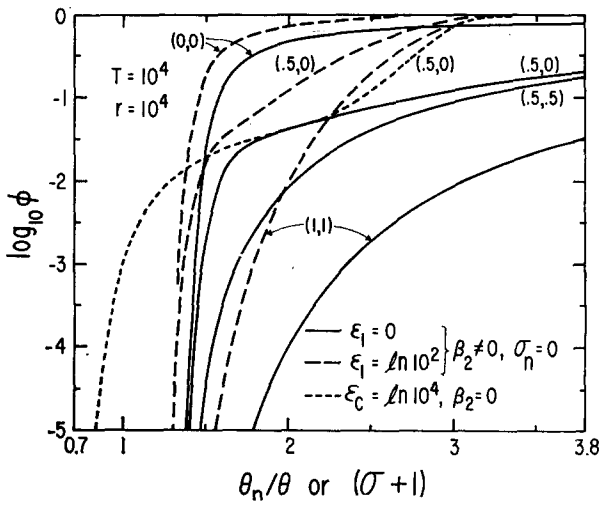

FIG. 11. Curves of $\log_{10}\phi$ vs (θ_n/θ) for $\beta_2=0$ or vs $(\sigma+1)$ for $\beta_2\neq 0$ for $T=10^4$ and several (ξ_1,ξ_2) combinations.

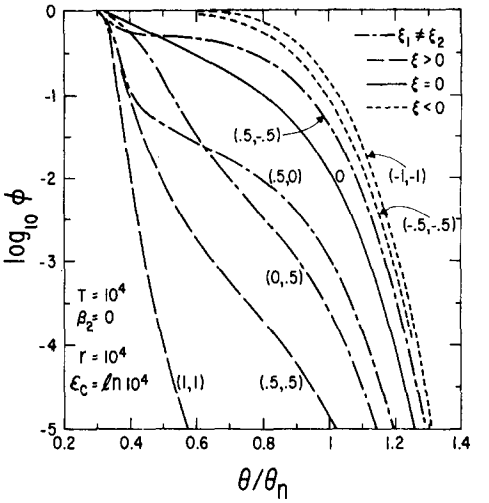

FIG. 12. Dependence of $\log_{10}\phi$ on (θ/θ_n) in the case $\beta_2=0$ for $T=10^4$ and several (ξ_1,ξ_2) combinations.

Also shown in Fig. 11 for the case $\beta_2\neq 0$ are corresponding curves for $\mathcal{E}_1=0$ (solid) and $\mathcal{E}_1>0$ (dashed). When $\mathcal{E}_1=0$ and $\xi_1\geq 0$, it will be noted that for a fixed time $T>0$, ϕ approaches unity slower than when $\mathcal{E}_1>0$ as σ increases and the temperature is lowered. In this case only, $bY=T$ is a constant independent of σ, otherwise, bY as well as Y and aY approach zero as σ increases at fixed T.

Since $\log_{10}\phi$ is usually presented plotted directly vs temperature in the stress relaxation case, Fig. 12 is so plotted for $\beta_2=0$, $T=10^4$, and several ξ_i combinations. The wedge-box curve (0.5,0) is in excellent qualitative agreement with experimental curves on polystyrene presented by Tobolsky.[49] Its detailed shape could, of course, be further altered by taking $T_c\neq T_1T_2$, by using ξ_i values somewhat different from (0.5,0), by altering r through a change in $\mathcal{E}_c$, or even by separating the wedge and box parts of the distribution so that there is a region of zero relaxation-time probability density between them.

ACKNOWLEDGMENT

The author is grateful to D. R. Powell for his careful computer programming work on the present problem.

[49] See reference 30, p. 72.